ACS OMEGA

http://pubs.acs.org/journal/acsodf

Article

Application of Multivariate Methods to Evaluate Differential Material Attributes of HPMC from Different Sources

Shulin Wan, Chuanyun Dai,* Yuling Bai, Wenying Xie, Tianbing Guan, Huimin Sun,* and Bochu Wang*

Cite This: *ACS Omega* 2021, 6, 28598−28610

Read Online

ACCESS | Metrics & More | Article Recommendations

ABSTRACT: The aim of the present study is to achieve differential material attributes (DMAs) of hydroxypropyl methylcellulose (HPMC) with different viscosity grades (K4M, K15M, and K100M) from different manufacturers (Anhui Shanhe and Dow Chemical). Two kinds of multivariate methods, principal component analysis (PCA) and orthogonal partial least squares discriminant analysis (OPLS-DA), were adopted. The physicochemical properties of HPMC were systematically investigated via various techniques (e.g., SEM, particle size detection, and SeDeM characterization). Data from 33 characterization variables were applied to the multivariate methods. The PCA and OPLS-DA results indicated the differences between the HPMC from two manufacturers by the common variables that include the tablet hardness (HD), tensile strength (TS), bulk density, interparticle porosity, Carr index, cohesion index, Hausner ratio, flowability, and the width of the particle size distribution (span). Interestingly, these variables showed a certain correlation with each other, supporting the characterization results. Except for these different variables of the HPMC obtained by multivariate analysis results, distinguishable shapes and surface morphologies also appeared between different sources. To sum up, the powder properties (particle size, surface topography, dimension, flowability, and compressibility) and the tablet properties (HD and TS) were recognized as the DMAs of HPMC samples. This work provided the multivariate methods for the physicochemical characterization of HPMC, with potential in the quality control and formulation development.

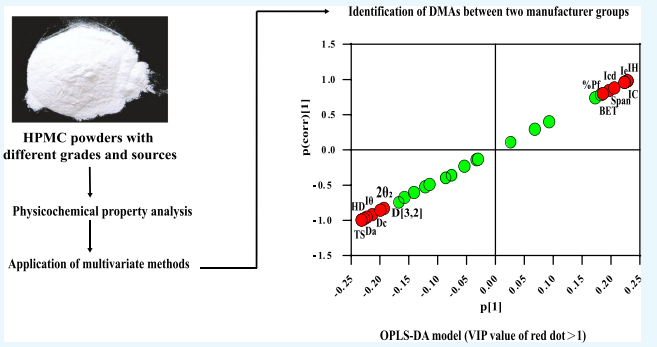

1. INTRODUCTION

The pharmaceutical development guideline in ICH Q8 (R2) stated that, as a pharmaceutical manufacturer, we should have an enhanced understanding of the product performance over a range of raw material attributes, manufacturing process options, and process parameters.[1] This guideline enucleates that material attributes are critical to drug development. To achieve the desired quality of the target product, the physical, chemical, and biological properties of the input material must be within an appropriate limit, range, or distribution.[2] These material attributes, which have a significant impact on product quality attributes, are treated as critical material attributes (CMAs). Compared with the drug substances, the CMAs of excipients are more difficult to find because they are confounding with the influence of active pharmaceutical ingredients (property and dose size),[3] formulations (composition, ratio),[4] the production process,[5] and so forth. The differential material attributes (DMAs) represent different properties between different materials, and their impact on product quality is not necessarily critical. This indicates that DMAs include CMAs, but DMAs are not necessarily CMAs.

Therefore, it is necessary to investigate the DMAs of input raw materials that may affect the performance of the output produced during the preformulation study.

Hydroxypropyl methylcellulose (HPMC) is the most commonly used hydrophilic matrix in the pharmaceutical industry owing to its nonionicity, nontoxicity, stability in different pH solutions, and cost-effectiveness.[6] To find out the DMAs of HPMC, many previous studies have examined the chemical,[7] mechanical,[8] and thermal[9] properties of HPMC, as well as the effects of viscosity, particle size, and other properties on drug release.[10] Recent types of research have investigated the relationship between the HPMC properties and the drug dissolution by using various new characterization methods, such as modulated differential scanning calorimetry

Received: June 8, 2021
Accepted: September 30, 2021
Published: October 21, 2021

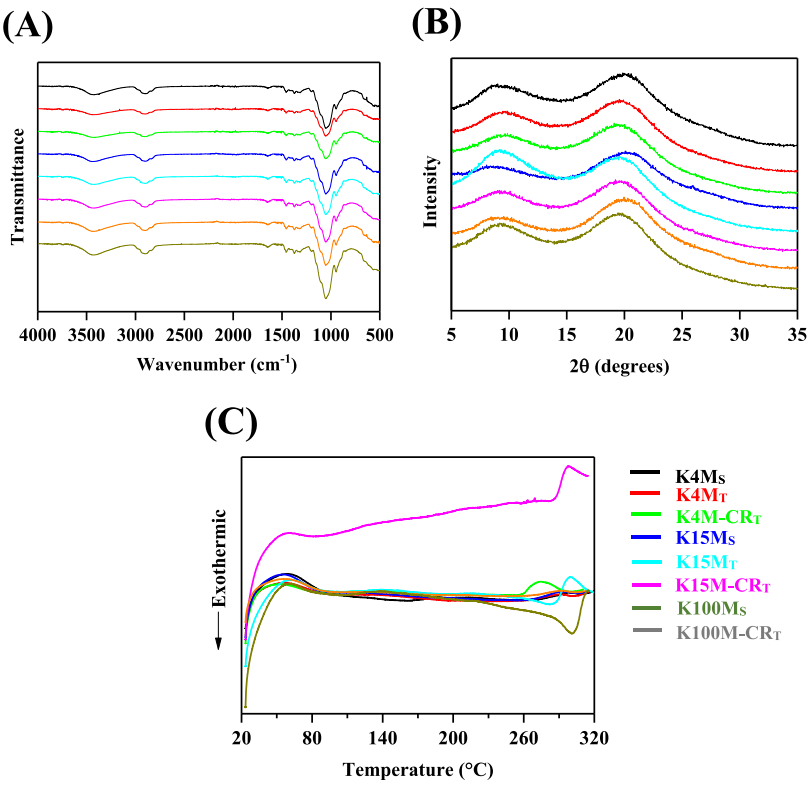

Figure 1. IR spectrums (A), PXRD diffractograms (B), and DSC traces (C) of HPMC powders. $K4M_S$, $K15M_S$, and $K100M_S$ represent three batches of HPMC with different viscosity grades from Anhui Shanhe Pharmaceutical Excipient Co., Ltd. (China). $K4M_T$, $K4M\text{-}CR_T$, $K15M_T$, $K15M\text{-}CR_T$, and $K100M\text{-}CR_T$ represent five batches of HPMC with different viscosity grades from Dow Chemical (USA). The viscosity of K4M, K15M, and K100M is 4000, 15,000, and 100,000 mPa·s, respectively.

(DSC)[11] nuclear magnetic resonance,[12] FTIR,[13] and statistical methods.[14] However, little is known about the systematic research of material attributes of HPMC.

Due to the differences in raw materials and preparation processes, many properties (e.g., particle size, density, powder flow, and compressibility, among others) of the HPMC produced by different manufacturers are also different. The impact of intervendor and inter-lot variability of the HPMC on drug release has also been found.[15] Commercially, the HPMC is divided into different viscosity and substitution grades according to pharmaceutically approved limits.[12] This implies that HPMC with the same grades from the same sources may have similar functionality and behavior. Indeed, the final products prepared by HPMC from different sources also exhibit a significant difference in the performance in vitro and in vivo.[15] Consequently, it is indispensable to systematically investigate DMAs of HPMC from different sources before the prescription.

Multivariate statistical analysis is often used in genomics, proteomics, and metabolomics research because it can better distinguish the differentials among different groups. Principal component analysis (PCA) is an unsupervised statistical method for rescreening and combining information from multivariate data, extracting new comprehensive variables with the best explanatory ability, and reflecting as much information as possible in the original variables.[16] Orthogonal partial least squares discriminant analysis (OPLS-DA) is a supervised discriminant analysis method, which separately trains the characteristics of different samples (such as observation samples and control samples), generates a training set, and tests the credibility of the training set.

In light of the abovementioned discussion, the performance indicators of eight batches of HPMC were statistically analyzed as independent variables. Furthermore, the SeDeM diagram and SEM characterization were used to explain the variation intuitively. The SeDeM method is a tool used to determine the compression performance and fluidity of materials.[17] Finally, multivariate analysis and characterization analysis were integrated to identify the DMAs of HPMC from different sources.

2. RESULTS AND DISCUSSION

2.1. IR, PXRD, DSC, and SEM. The IR spectrums (Figure 1A and Table 1) illustrated an absorption peak at 3420.46−3446.46 cm^{-1} identifying the −OH group, which is part of the polymer. An absorption peak was also determined at 2897.18−2901.03 cm^{-1} identifying the presence of the $-CH_2$ group. Another absorption peak at 1050.42−1053.3 cm^{-1} was determined, which is the characteristic of the −CO− group. The HPMC powders revealed the same absorption peak at the same wavenumber position, and no peak appeared at other positions, indicating that their molecular structure did not change.

In powder X-ray diffractograms (Figure 1B and Table 1), the 2θ values of different HPMC samples ranged from 9.2 to 9.7 and 19.3 to 20.1°, demonstrating distinct sharp, intense peaks. The positions of the two diffraction peaks were very similar, indicating that the eight batches of HPMC showed a polymorphic structure, and the crystal structure did not change significantly.

The DSC traces (Figure 1C and Table 1) representing reverse heat flow signals revealed the same trend among

https://doi.org/10.1021/acsomega.1c03009
ACS Omega 2021, 6, 28598−28610

Table 1. Experimental Values of HPMC Variables for Multivariate Statistical Analysis[a]

			HPMC (different grades and sources)							
incidence	parameter	unit	$K4M_S$	$K4M_T$	K4M-CR_T	$K15M_S$	$K15M_T$	K15M-CR_T	$K100M_S$	K100M-CR_T
FTIR	σ_1	cm^{-1}	3423.510	3423.060	3420.310	3446.460	3420.400	3420.960	3420.700	3420.460
	σ_2	cm^{-1}	2900.680	2901.030	2899.960	2899.940	2897.180	2900.500	2900.380	2899.720
	σ_3	cm^{-1}	1050.810	1051.090	1053.300	1051.440	1051.900	1050.590	1053.450	1050.420
XRD	$2\theta_1$	°	9.676	9.702	9.231	9.493	9.257	9.571	9.833	9.205
	$2\theta_2$	°	19.606	19.370	19.475	20.078	19.239	19.527	19.947	19.396
DSC	T_g	°C	284.459	280.549	272.333	281.851	293.803	297.051	285.265	301.863
particle size of HPMC powders	d_{10}	μm	43.550	29.550	27.150	36.400	32.350	29.650	42.600	27.000
	d_{50}	μm	93.150	83.850	82.750	97.100	104.500	84.550	99.850	77.600
	d_{90}	μm	179.000	182.000	179.000	187.000	209.000	203.000	186.000	188.000
	D[3,2]	-	67.550	49.650	45.350	60.700	59.200	51.300	65.000	44.800
	D[4,3]	-	104.500	96.850	93.950	105.500	125.000	103.000	108.000	95.050
	BET	m^2/kg	65.090	86.910	95.210	71.200	72.950	84.150	66.510	96.400
	span	-	1.454	1.818	1.829	1.551	1.686	2.050	1.436	2.075
	width	μm	135.500	152.500	151.400	150.600	176.200	173.400	143.400	161.000
nozzle atomization particle size	d_{V10}	μm	36.872	39.293	42.452	41.020	42.383	36.417	43.952	45.077
	d_{V50}	μm	72.683	66.665	72.253	71.082	72.479	64.950	84.023	81.215
	d_{V90}	μm	143.213	113.152	122.923	122.935	124.057	115.837	160.315	146.034
	S	-	1.463	1.108	1.114	1.152	1.127	1.223	1.380	1.243
SeDeM index	% Pf	-	14.650	25.650	27.150	18.900	21.450	26.200	15.150	29.950
	$I\theta$	-	0.006	0.004	0.004	0.006	0.004	0.004	0.007	0.003
	Da	g/mL	0.411	0.293	0.306	0.421	0.301	0.301	0.425	0.279
	Dc	g/mL	0.589	0.479	0.487	0.597	0.500	0.472	0.617	0.459
	Ie	-	0.737	1.325	1.219	0.700	1.321	1.201	0.732	1.402
	IC	-	30.250	38.800	37.250	29.450	39.800	36.200	31.100	39.100
	Icd	-	120.400	233.500	212.200	101.400	243.000	221.200	96.200	258.500
	IH	-	1.434	1.634	1.594	1.418	1.660	1.568	1.452	1.644
	α	°	38.500	46.650	43.650	40.000	46.000	46.650	39.650	46.850
	t''	s	10.140	45.000	15.060	7.940	40.300	21.740	7.080	25.700
	% HR	%	2.780	4.090	3.760	3.200	3.300	4.490	2.990	4.060
	% H	%	12.400	10.540	10.120	10.720	9.760	9.080	10.340	8.520
tablet property	HD	N	63.379	28.704	33.514	65.349	26.818	27.619	66.623	26.666
	TS	N/mm^2	1.365	0.693	0.765	1.375	0.649	0.639	1.403	0.655
viscosity	vis	mPa·s	3286.667	3133.334	3896.667	12,600.000	13,466.667	15,433.334	71,800.000	77,500.000

[a]The results are an average of at least three measurements. $K4M_S$, $K15M_S$, and $K100M_S$ represent three batches of HPMC with different viscosity grades from Anhui Shanhe Pharmaceutical Excipient Co., Ltd. (China). $K4M_T$, K4M-CR_T, $K15M_T$, K15M-CR_T, and K100M-CR_T represent five batches of HPMC with different viscosity grades from Dow Chemical (USA). The viscosity of K4M, K15M, and K100M is 4000, 15,000, and 100,000 mPa·s, respectively.

different HPMC samples. The HPMC samples exhibited obvious variations in the heat flow from 20 to 80 °C, which is mainly caused by the removal of adsorbed water and bound water from solid materials.[18] Except for K100M-CR_T, other samples had an endothermic peak at 260−280 °C, which may be caused by the content difference of methoxy and hydroxypropyl among HPMC samples with different viscosity grades. The glass transition temperature (T_g) of HPMC was significantly different in the range of 280−300 °C. It can be speculated that HPMC, as an amorphous polymer, may have both melting and crystalline area destruction during the thermal effect of HPMC, as well as phenomena such as decomposition and loss of water dispersion.[19]

The SEM images (Figure 2) showed the distinguishable shape and surface morphology of HPMC powders from two manufacturers. Most particles in the majority around 100 μm, except K15M, were observed according to the images. Physical shapes of HPMC from Anhui Shanhe were striped and smooth on the surface, while those of HPMC from Dow Chemical were layered sheet-like structures with a rough surface. The powder particles appeared quite smooth on the surface, showing excellent powder flowability.

2.2. Particle Size Distribution. As shown in Figure 3 and Table 1, there were significant differences in the particle size of HPMC powders. K15M had a higher particle size (d_{10}, d_{50}, and d_{90}) compared to HPMC samples with different viscosity grades. On the other hand, the obvious coarse powders of $K15M_T$ (d_{50} and d_{90}) were discovered in the same viscosity grades. Of note, the values of d_{10}, d_{50}, and d_{90} of Dow Chemical samples increased in the following order: K100M-CR_T < K4M-CR_T < K15M-CR_T. The particle sizes (d_{10}, d_{50}, d_{90}, span, and width) of Anhui Shanhe samples were larger than those of Dow Chemical samples. On the contrary, the smallest BET for Anhui Shanhe samples indicated distinctive surface topography caused by manufacturers, supporting the SEM observations. BET is the most crucial characteristic of powders due to its influence on other properties of powders (such as solubility and adsorption).[20] The larger powders ($K15M_T$) had the lowest BET (72.95 kg m^{-2}), whereas the smaller ones (K100M-CR_T) had the highest BET (96.4 kg m^{-2}), which

https://doi.org/10.1021/acsomega.1c03009
ACS Omega 2021, 6, 28598−28610

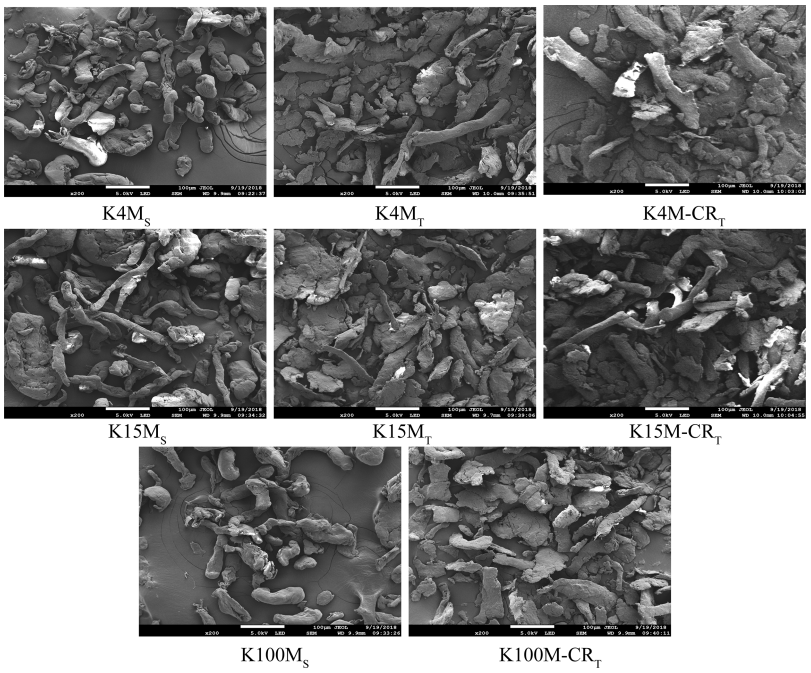

Figure 2. SEM images of HPMC powders under 200x magnification. K4M$_S$, K15M$_S$, and K100M$_S$ represent three batches of HPMC with different viscosity grades from Anhui Shanhe Pharmaceutical Excipient Co., Ltd. (China). K4M$_T$, K4M-CR$_T$, K15M$_T$, K15M-CR$_T$, and K100M-CR$_T$ represent five batches of HPMC with different viscosity grades from Dow Chemical (USA). The viscosity of K4M, K15M, and K100M is 4000, 15,000, and 100,000 mPa·s, respectively. The SEM photographs were taken by Shulin Wan.

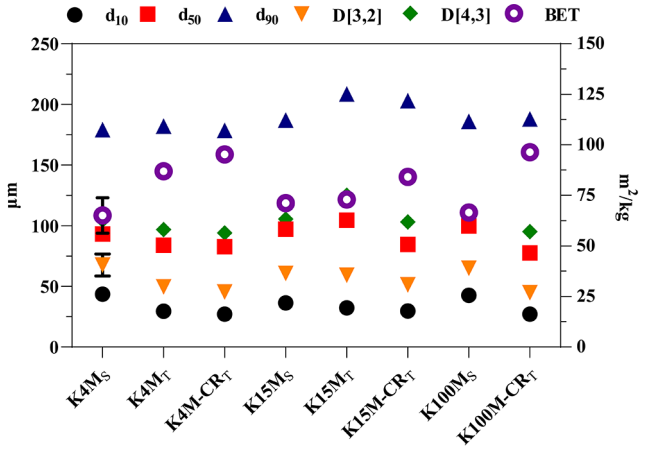

Figure 3. Particle size distribution of HPMC powders (n = 3, $\bar{X} \pm$ SD). K4M$_S$, K15M$_S$, and K100M$_S$ represent three batches of HPMC with different viscosity grades from Anhui Shanhe Pharmaceutical Excipient Co., Ltd. (China). K4M$_T$, K4M-CR$_T$, K15M$_T$, K15M-CR$_T$, and K100M-CR$_T$ represent five batches of HPMC with different viscosity grades from Dow Chemical (USA). The viscosity of K4M, K15M, and K100M is 4000, 15,000, and 100,000 mPa·s, respectively.

confirmed that the BET of the powder was negatively related to the particle size and positively related to the porosity.

The nozzle atomization particle size results of HPMC aqueous solutions are shown in Table 1. The values of d_{v10}, d_{v50}, and d_{v90} of Dow Chemical samples with different viscosity grades increased in the following order: K4M$_T$ < K15M$_T$ < K100M-CR$_T$. In contrast to Dow Chemical, the nozzle atomization particle sizes (d_{V10}, d_{V50}, and d_{V90}) of HPMC aqueous solutions from Anhui Shanhe were larger, which was consistent with the particle size results. At the same time, the particle size distribution span (S) also showed the same trend. The smaller the S, the narrower the atomized particle size distribution and the smaller the consistency. The viscosity of HPMC aqueous solutions is mainly affected by three aspects: the degree of polymerization of the product, the concentration of the product in the aqueous solution, and the temperature of the solution. When the concentration of HPMC aqueous solutions increased to 1% in the pre-experiment, their viscosities were too large and the peristaltic pump could not deliver liquid. Thus, 0.5% HPMC was selected as the research condition of nozzle atomization particle size in this study.

2.3. SeDeM Diagram. The diagram visually shows the advantages and defects of the different physical properties of pharmaceutical powders. The SeDeM diagram is composed of 12 parameters to form an irregular 12-sided polygon with a radius of 10. According to the conversion formula, the experimental value of each parameter was converted into the corresponding radius value using the SeDeM method. In order to quantitatively evaluate whether HPMC is suitable for direct compression, the following indexes (IP, IPP, and IGC) were calculated

$$\text{parameter index (IP)} = \frac{\text{no. } P \geq 5}{\text{no. Pt}} \quad (1)$$

$$\text{parameter index (IPP)} = \text{mean radius of all parameters} \quad (2)$$

$$\text{good compressibility index (IGC)} = \text{IPP} \times f \quad (3)$$

where no. $P \geq 5$ is the number of parameters with values equal to or more than 5 and no. Pt is the total number of parameters. f is the reliability factor (0.952), which is the ratio of the 12-sided area to the circular area. The acceptability limits would correspond to IP $\geq$ 0.5, IPP $\geq$ 5, and IGC $\geq$ 5.

Significant similarities among the SeDeM diagrams of the same manufacturer were observed in Figure 4. Additionally,

https://doi.org/10.1021/acsomega.1c03009
ACS Omega 2021, 6, 28598−28610

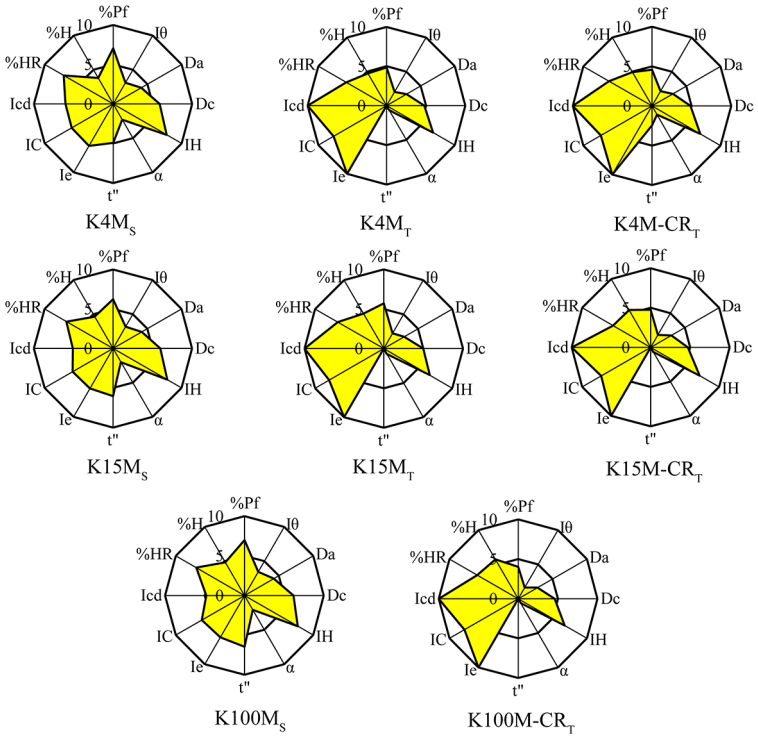

Figure 4. SeDeM diagram with 12 parameters of HPMC powders. K4M$_S$, K15M$_S$, and K100M$_S$ represent three batches of HPMC with different viscosity grades from Anhui Shanhe Pharmaceutical Excipient Co., Ltd. (China). K4M$_T$, K4M-CR$_T$, K15M$_T$, K15M-CR$_T$, and K100M-CR$_T$ represent five batches of HPMC with different viscosity grades from Dow Chemical (USA). The viscosity of K4M, K15M, and K100M is 4000, 15,000, and 100,000 mPa·s, respectively.

Dow Chemical samples were superior in compression performance [interparticle porosity (Ie), Carr index (IC), and cohesion index (Icd)] compared to Anhui Shanhe samples. However, the powder flow of all HPMC samples was defective, especially the angle of repose (α) and flowability (t''). As listed in Table 2, the compressibility results showed that IP, IPP, and IGC of Anhui Shanhe samples were all in line with the acceptability limit, revealing that they had good compressibility and could be used for direct compression. However, Dow Chemical samples with defective compressibility could be supplemented with suitable excipients to make up for their deficiency due to the lower values of IP, IPP, and IGC in the range of 0.42−0.67, 5−5.27, and 4.76−5.08, respectively. The compressibility of Anhui Shanhe samples was superior to Dow Chemical samples in the same viscosity grades, corresponding to the larger values of IP, IPP, and IGC.

The SeDeM expert system, as a tool for predicting the compression characteristics of pharmaceutical excipients, was used to quantitatively and intuitively diagnose the differences of HPMC powder properties from different sources in this work. The more indicators the SeDeM expert system contains, the richer the quality information of the excipients and the higher the reliability. Thus, 12 indicators and 3 parameters (IP, IPP, and IGC) commonly utilized in the SeDeM method were used to comprehensively investigate the flowability and compression characteristics of HPMC in this experiment. The SeDeM results showed that the powder flow and compression of Anhui Shanhe samples were superior to Dow Chemical samples because of their larger particle size and smooth surface. Flowability and compressibility affecting the continuous and stable delivery of materials in the process of tablet compression are two principal properties. Materials with defective flowability will lead to uneven content and large weight differences of the final product in the process of transportation. Therefore, it is very important to study the powder performance of materials before prescription, especially flowability and compression.

2.4. Tablet Properties. The remarkable differences in tablet properties of HPMC between different sources are highlighted in Table 1. Tablet hardness (HD) and tensile strength (TS) of Anhui Shanhe samples were greater than those of Dow Chemical samples, which was similar to the compressibility and SEM results. Furthermore, compared to HPMC powders from different sources with the same viscosity grade, HD and TS of Anhui Shanhe samples were both greater than those of Dow Chemical samples, suggesting that powder tabletability was better. HPMC with better powder tabletability not only has greater mechanical strength in the preparation of tablets but also has the advantages of easy production, storage, and transportation.

2.5. PCA Model. The components with the greatest contribution to the difference of data were gained by data dimensionality reduction in the PCA by maintaining the characteristics of the original data as much as possible without grouping the samples before the process of analysis.[21] In this work, the design matrix was composed of 8 observations (representing 8 batches of HPMC with 3 viscosity grades from 2 manufacturers) with 33 variables (33 physicochemical properties of HPMC). First, a 33-dimensional variable space was constructed, where each variable represented an axis. Then, each observation in the matrix was placed in the 33-dimensional variable space and projected into a point in the space. Finally, the direction with the largest distance between the data points was found in the multidimensional space,

https://doi.org/10.1021/acsomega.1c03009
ACS Omega 2021, 6, 28598−28610

Table 2. Radius Parameters, Mean Incidence, and Parametric Index of SeDeM Characterization of HPMC Powders[a]

samples	parameter (radius value)										factor				index	
	Da	Dc	Ie	IC	Icd	IH	α	t''	% HR	% H	% Pf	Iθ	dimension	compressibility	power flow	stability	lubricity	IP	IPP	IGC
$K4M_S$	4.11	5.89	6.14	6.05	6.02	7.83	2.30	4.93	7.22	3.80	7.07	3.10	5.00	6.07	5.02	5.09	5.51	0.58	5.37	5.11
$K4M_T$	2.93	4.79	10.00	7.76	10.00	6.83	0.67	0.00	5.91	4.73	4.87	2.04	3.86	9.25	2.50	5.32	3.46	0.42	5.04	4.80
$K4M\text{-}CR_T$	3.06	4.87	10.00	7.45	10.00	7.03	1.27	2.47	6.24	4.94	4.57	2.14	3.97	9.15	3.59	5.59	3.36	0.42	5.34	5.08
$K15M_S$	4.21	5.97	5.83	5.89	5.07	7.91	2.00	6.03	6.80	4.64	6.22	3.20	5.09	5.60	5.31	5.72	4.71	0.67	5.31	5.05
$K15M_T$	3.01	5.00	10.00	7.96	10.00	6.70	0.80	0.00	6.70	5.12	5.71	2.22	4.01	9.31	2.50	5.91	3.97	0.67	5.27	5.02
$K15M\text{-}CR_T$	3.01	4.72	10.00	7.24	10.00	7.16	0.67	0.00	5.51	5.46	4.76	1.83	3.87	9.08	2.61	5.49	3.29	0.50	5.10	4.86
$K100M_S$	4.25	6.17	6.10	6.22	4.81	7.74	2.07	6.46	7.01	4.83	6.97	3.45	5.21	5.71	5.42	5.92	5.21	0.58	5.51	5.24
$K100M\text{-}CR_T$	2.79	4.59	10.00	7.82	10.00	6.78	0.63	0.00	5.94	5.74	4.01	1.64	3.69	9.27	2.47	5.87	2.83	0.50	5.00	4.76

[a]The results are an average of at least three measurements. $K4M_S$, $K15M_S$, and $K100M_S$ represent three batches of HPMC with different viscosity grades from Anhui Shanhe Pharmaceutical Excipient Co., Ltd. (China). $K4M_T$, $K4M\text{-}CR_T$, $K15M_T$, $K15M\text{-}CR_T$, and $K100M\text{-}CR_T$ represent five batches of HPMC with different viscosity grades from Dow Chemical (USA). The viscosity of K4M, K15M, and K100M is 4000, 15,000, and 100,000 mPa·s, respectively.

which was regarded as the principal component (PC). Recombinant variables contributed most to the differences between observations. The line closest to the data was determined based on the least square method, and each observation was projected onto the line to produce coordinate values (fractions) along the PC line.[4] Moreover, a second PC orthogonal to the first PC was derived when the previous component was not sufficient to model a system change of the data set.

The suitability of PCA was assessed prior to the analysis using cross-validation. The R^2X value describes the cumulative interpretation rate of the model in the x-axis direction, while the Q^2 value describes the cumulative prediction rate of the model by cross-validation. The closer each value is to 1.0, the better the fit of the model. As listed in Table 3, R^2X was greater than 0.5 and Q^2 was close to 0.5, which indicated that the accuracy of the PCA model and the explanatory ability of each PC to the corresponding variable were all within the acceptable range.

Table 3. Validation of the PCA and OPLS-DA Models[a]

model	component	R^2X	R^2Y	Q^2	difference
PCA	1	0.572		0.388	
	2	0.706		0.326	
OPLS-DA	1	0.652	0.826	0.943	0.117
	2	0.558	0.799	0.862	0.083

[a]R^2X and R^2Y refer to the cumulative explained variance and Q^2 refers to the cumulative explained variance for modeling in cross-validation. There is a difference between R^2Y and Q^2.

In the left and right quadrants of the score plot (Figure 5A), along with the first PC, eight batches of HPMC were grouped; the manufacturer was one of the parameters resulting in the clear separation of the two groups. Interestingly, $K15M_T$ was present in the group of Dow Chemical samples and was completely separated from other ones, supporting the coarse particle size results. To appreciate the underlying variables that are indicative of the grouping, the loading plots were further evaluated. The loading plot not only shows the contribution degree of each variable to the corresponding but also expounds on the correlation between variables.[22] The samples and variables on the same side and in the same direction along the coordinate axis of PCs are positively correlated, but the ones on two sides of the diagonal position of the origin are negatively correlated. As depicted in Figure 5B, the first and second PCs {p[1] and p[2], respectively} explained 52.7 and 13.3%, respectively, of the overall variability in the data set, accounting for 70.5% of the total variation. Apparently, the loading vectors of variables such as "HD, TS, bulk density (Da), tapped density (Dc), Ie, IC, Icd, Hausner ratio (IH), α, % Pf, and span," which were strongly correlated with the first PC, could be regarded as being crucial for the differentiation. In addition, the variables HD and TS were positively correlated with Da, Dc, d_{10}, and d_{50} along with the first PC and inversely correlated to Ie, IC, Icd, α, IH, % Pf, span, and d_{90} on two sides of the diagonal position of the origin. This means that high particle size and dimension as well as both low compressibility and high flowability correlate to high tablet mechanical strength. BET was negatively correlated with small particle size variables (d_{10} and d_{50}), whereas positively correlated with Ie, which was in agreement with the powder size distribution

https://doi.org/10.1021/acsomega.1c03009
ACS Omega 2021, 6, 28598−28610

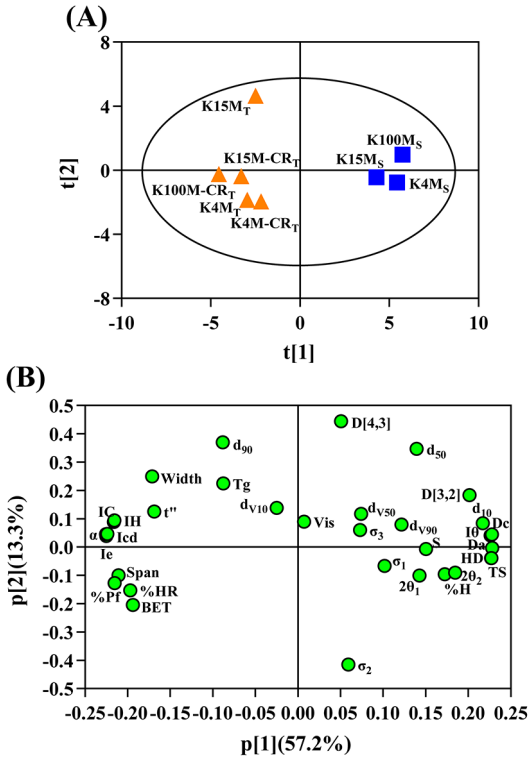

Figure 5. Score plot (A) and loading plot (B) of the PCA model for HPMC samples from two manufacturer groups. K4M$_S$, K15M$_S$, and K100M$_S$ represent three batches of HPMC with different viscosity grades from Anhui Shanhe Pharmaceutical Excipient Co., Ltd. (China). K4M$_T$, K4M-CR$_T$, K15M$_T$, K15M-CR$_T$, and K100M-CR$_T$ represent five batches of HPMC with different viscosity grades from Dow Chemical (USA). The viscosity of K4M, K15M, and K100M is 4000, 15,000, and 100,000 mPa·s, respectively.

results of HPMC, suggesting that PCA can better enucleate the correlation between variables.

2.6. OPLS-DA Model. A supervised OPLS-DA was also carried out to enhance the separation between HPMC samples. This method divides observations into different groups via manual operation, filters out the noise interference that has nothing to do with the grouping to the greatest extent, and concentrates the most relevant factors on the first PC, which can more accurately reflect the differences between groups. The prediction reliability of OPLS-DA was evaluated prior to the analysis by cross-validation. The closer the three parameters (R^2X, R^2Y, and Q^2) involved in OPLS-DA are to 1, the better the fitting effect of the model. R^2X and R^2Y represent the interpretation rate of the model along with the X and Y matrix directions, respectively. Q^2 is used to evaluate the predictive ability of the model. As listed in Table 3, the values of coefficients R^2X = 0.652, R^2Y = 0.826, and Q^2 = 0.943 are all good because they are all above 0.5, and the difference between R^2Y and Q^2 is 0.117, which is satisfactory as it is lower than 0.2−0.3. The OPLS-DA model had a better classification effect than the PCA model. As shown in Table 4, the high percentage of correct classification rate (CCR), sensitivity, and specificity (100%) in the confusion matrix further revealed the consistency between the predicted classification of the OPLS-DA model and the actual classification.

The preliminary OPLS-DA score plot showed that a good and clear separation was attained between the samples (Figure 6A). Besides, HPMC samples from the same factory also showed a performance difference to a certain extent along with the second PC. The *S*-plot based on the OPLS-DA model is used to screen components that are strongly correlated with

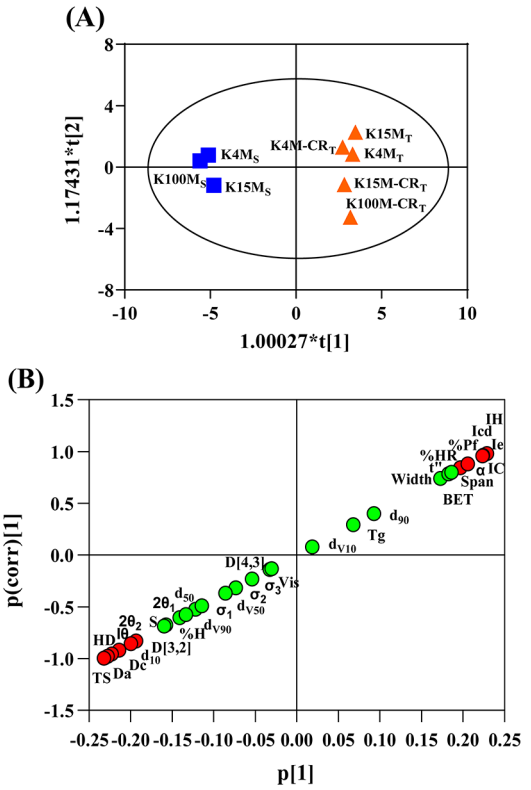

Figure 6. Score plot (A) and *S*-plot (B) of the OPLS-DA model for HPMC samples from two manufacturer groups. The VIP value of the red dot in the *S*-plot is greater than 1. K4M$_S$, K15M$_S$, and K100M$_S$ represent three batches of HPMC with different viscosity grades from Anhui Shanhe Pharmaceutical Excipient Co., Ltd. (China). K4M$_T$, K4M-CR$_T$, K15M$_T$, K15M-CR$_T$, and K100M-CR$_T$ represent five batches of HPMC with different viscosity grades from Dow Chemical (USA). The viscosity of K4M, K15M, and K100M is 4000, 15,000, and 100,000 mPa·s, respectively.

Table 4. Confusion Matrix of the OPLS-DA Model[a]

	predicted class							
confusion matrix	Shanhe	Dow	samples	% NER	% CCR (%)	sensitivity (%)	specificity (%)	samples (%)
actual class	Shanhe	3	0	3	100			
	Dow	0	5	5	100			
total				8	100	100	100	100

[a]Nonerror rate (% NER) for each class = 100 × (correctly classified)/(total), correct classification rate (% CCR) for all classes = 100 × (correctly classified)/(total), sensitivity = % of samples of class *i*, correctly classified as *i*, and specificity = % of samples of class ≠ *i*, correctly classified as not i.

https://doi.org/10.1021/acsomega.1c03009
ACS Omega 2021, 6, 28598−28610

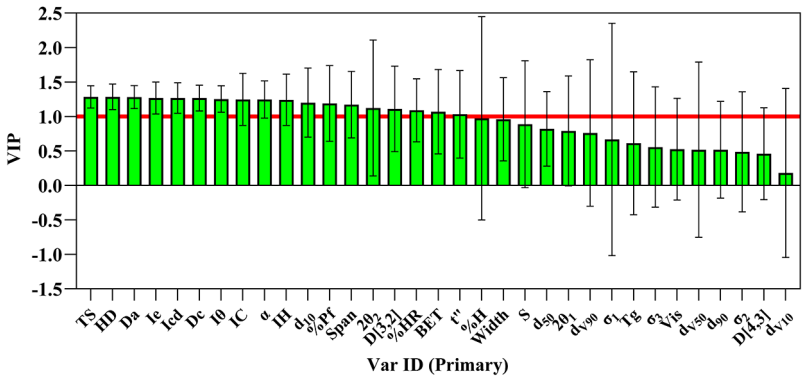

Figure 7. VIP indexes of all variables based on the OPLS-DA model (n = 3, $\bar{X}$±SD). The red lines are the threshold equal to 1.

PCs, and the further away they are from the origin, the greater their contribution value to the score plot. As shown in the *S*-plot (Figure 6B), some variables (HD, TS, Da, Ie, IC, Icd, and IH) contributed more to their classification than other variables. Furthermore, variable importance in projection (VIP) indexes of all variables based on the OPLS-DA model were further used to evaluate the importance of all independent variables, corresponding to differential variables. The VIP values of some variables (HD, TS, Da, Ie, IC, Icd, IH, α, d_{10}, Iθ, % Pf, span, BET, D [3, 2], % HR, and $2\theta_2$) were all greater than 1 (Figure 7), which showed that these variables were crucial for the differentiation.

The common variables, including "HD, TS, Da, span, Ie, IC, Icd, IH, and α," which could effectively distinguish the differences among HPMC samples from two manufacturers, were probed based on PCA and OPLS-DA models. We proposed that the particle size (span), dimension (Da), flowability (IH and α), compressibility (Ie, IC, and Icd), and tablet properties (HD and TS) were identified as the DMAs of HPMC, consistent with HPMC characterization results. This indicated the good feasibility of multivariate statistics for evaluating the DMAs of HPMC. Moreover, there was no similar surface morphology of HPMC from two manufacturers observed by SEM by excluding the common variables obtained by multivariate statistics. Thus, the results showed that HPMC from different sources was mainly differentiated by two overarching properties, namely the powder properties (particle size, surface topography, dimension, flowability, and compressibility) and the tablet properties (HD and TS), which were assessed as the DMAs of HPMC. In this study, the preliminary identification of these DMAs is of great significance for the quality control and quality evaluation of HPMC. In the concept of pharmaceutical quality by design, the CMAs derived from the critical quality attributes of products can be definitely benefited from the systematic study of the DMAs. Further verification in follow-up research is required to determine whether these DMAs are the CMAs affecting HPMC preparation products.

The multivariate methods gave satisfactory results for other pharmaceutical excipients proving their effectiveness. Haware et al.[22] evaluated data from the basic powder characteristics as well as the compression characteristics of four excipients by PCA. The results showed that these excipients were grouped, and the variables that have a significant impact on the grouping had a certain correlation. Siow et al.[4] identified the differences between samples using the PCA model constructed by 18 physical properties (variables) of 18 batches of co-freeze-dried mannitol-HPMC tableting excipients (observation samples) and understood the underlying variables (bulk fill-related properties, compression behavior-related properties, and flow-related properties) that contributed to the differences. The suitability of the PCA model was assessed by cross-validation before analysis, and no external validation (additional freeze-dried mannitol-HPMC excipients) was carried out. OPLS-DA has been widely used in the identification of the chemical markers of traditional Chinese medicine and its compound prescriptions, as well as the identification of biomarkers in metabolomics in recent years.[23−25] Validation of an analysis model is critical for multivariate statistical analysis. It usually requires an external validation with a training data set and test data set, but in cases with few actual samples and large statistical data, external validation may not be demanded. In this research, cross-validation without external verification (additional HPMC lots) was carried out in the PCA and OPLS-DA models due to the fewer samples. The interpretation rate and predictive ability of the model were satisfactory in terms of a good discrimination rate, owing to the values of R^2 and Q^2. Moreover, the prospect of this study is to use the model as an auxiliary tool to identify HPMC, preliminarily explore the differences of characterization data, and not only rely on the model to obtain very perfect prediction results. The present study has its limitation in terms of external model validation, but this did not affect the identification of the DMAs of HPMC using the models. This work is a pre-study that should be continued in order to increase the database on HPMC and evaluate the DMAs of HPMC from different sources. In future, similar studies must test more HPMC samples per variety and source to better verify the multivariate statistical model. Therefore, multivariate statistics can effectively and quickly mine useful information from massive data generated using numerous technologies, which is advantageous to quality evaluation and quality control of HPMC.

3. CONCLUSIONS

In this work, the physicochemical characterization combined with PCA and OPLS-DA models was applied to analyze HPMC samples from different sources. Both the PCA and OPLS-DA models showed good discrimination and classification for HPMC samples, and the OPLS-DA model has a better classification effect than the PCA model. In addition, the loading plots in PCA and *S*-plots in OPLS-DA clearly demonstrated that some variables (HD, TS, Da, span, Ie, IC, Icd, IH, and α) had a much more significant contribution than

https://doi.org/10.1021/acsomega.1c03009
ACS Omega 2021, 6, 28598−28610

other variables for the differentiation of HPMC samples from different sources. Interestingly, these variables showed a certain correlation with each other, supporting the characterization results. The integrated results of material characterization and multivariate analysis indicated that particle size (span), surface topography, dimension (Da), flowability (IH and α), compressibility (Ie, IC, and Icd), and tablet properties (HD and TS) were evaluated as the DMAs of HPMC. Multivariate data analysis intelligently clarifies the internal relationship between the performance parameters of materials, avoiding the fact that evaluation of material properties is often empirical and the decision-making processes are experience-based. The results suggested that the multivariate methods have the potential to contribute to identifying the difference in HPMC samples from different sources and find the latent variables that have a significant impact on the difference.

4. MATERIALS AND METHODS

4.1. HPMC Samples. HPMC K4M (lot no. 160221), K15M (lot no. 160426), and K100M (lot no. 160506) were obtained from Anhui Shanhe Pharmaceutical Excipient Co., Ltd. (China), and they were referred to as $K4M_S$, $K15M_S$, and $K100M_S$, respectively. HPMC K4M (lot no. D180G34001), K4M CR (lot no. D180G2T002), K15M (lot no. D180G4H002), K15M CR (lot no. D180FAE002), and K100M CR (lot no. D180F6E002) were obtained from Dow Chemical (USA), and they were referred to as $K4M_T$, K4M-CR_T, $K15M_T$, K15M-CR_T, and K100M-CR_T. Depending on the length of the chain or the increase in the molecular weight,[4] the order of the HPMC viscosity is as follows: K100M (100,000 mPa·s) > K15M (15,000 mPa·s) > K4M (4000 mPa·s). In designating the viscosity of the commercial HPMC, the letter "M" represents a multiplier of 1000 and the suffix "CR" stands for the controlled-release grade.[26] In the commercial HPMC manufactured by the Dow Chemical Company, the first part is a letter (E, F, or K) that relates to the degree of substitution, and controlled-release dosage forms mainly use the K or E grades of HPMC. The K grades (HPMC 2208) have a methoxy substitution of 19−24% and a hydroxypropyl substitution of 7−12%.

4.2. Characterization of Solid-State Properties. *4.2.1. Infrared Spectroscopy.* The appropriate amount of HPMC samples is ground into a fine powder in an agate mortar and mixed evenly with dried potassium bromide powder (the ratio is about 1: 100). The mixture was pressed into transparent samples about 1 mm thick and tested by a Fourier transform infrared spectrometer [Nicolet iS50, Thermo Fisher Scientific (China) Co., Ltd., USA]. The pressure is about 5 T/cm^2. The pressurization time should be maintained as at least 1 min.

4.2.2. Powder X-ray Diffraction. PXRD was carried out with a microfocus spot single crystal diffractometer (SuperNova, Agilent Technology Co., Ltd., Poland), and Cu Kα radiation (λ = 1.54 Å) was used as the X-ray source. The sample was pretreated by this method that was placed into a sample holder and pressed by a glass slide to ensure coplanarity between surfaces of the powder and the sample holder.[27] Then, the sample was scanned over the 2θ range of 5−35° with a step size of 0.04°/s, an operating condition with a voltage of 50 kV, and a current of 35 mA.

4.2.3. Differential Scanning Calorimetry. Thermograms of HPMC samples were recorded by using a flow differential scanning calorimeter [DSC404F3, NETZSCH Instrument (Shanghai) Co., Ltd., Germany]. Calibration of the instrument was carried out using indium and zinc as standards.[28] Selected samples (about 5 mg) were placed into standard aluminum pans, sealed, and pierced to provide three vent holes.[29] Scanning was performed with a heating rate of 10 °C/min from 20 to 320 °C under argon purge of 50 mL/min and argon protection of 20 mL/min.

4.2.4. Scanning Electron Microscopy. The HPMC samples were coated with a thin layer of platinum (thickness ∼50 Å) using an ion-beam sputter (JEC-3000FC, JEOL Co., Ltd., Japan) for 4 min at 8×10^{-3} MPa, 15 mA current, and 100% turbo speed. The surface morphology of the coated particles was observed using SEM (JSM-7800F, JEOL Co., Ltd., Japan) at a magnification of 200 times with an accelerating voltage of 5.0 kV and a spot size of 3.0 under EBSD mode.

4.3. Particle Size Distribution. *4.3.1. Particle Size of HPMC Powders.* The particle size of HPMC powders was determined by a dry method using a laser diffraction particle size analyzer (Mastersizer 3000, Malvern Instruments Co., Ltd., England). Approximately 5 g of the powder was delivered continuously with dry vibrating powder dispersion and maintained at about 0.2 MPa to make the dispersion of the powders effective. The refractive index and absorbance of HPMC are 1.34 and 0.01, respectively. From the measured size distribution, D[3,2], D[4,3], d_{90}, d_{50}, d_{10}, and BET were derived. The span (width of particle size distribution) and the width (range of particle size distribution) were calculated by using the following formula[28]

$$\text{span} = \frac{d_{90} - d_{10}}{d_{50}} \tag{4}$$

$$\text{width} = d_{90} - d_{10} \tag{5}$$

where d_{90}, d_{50}, and d_{10} represent the particle diameter corresponding to the cumulative particle distribution score of 90, 50, and 10%, respectively. D[3,2], D[4,3], and BET represent the surface area mean diameter, the volume-weight mean diameter, and the specific surface area, respectively. Each measurement was conducted in triplicate.

4.3.2. Nozzle Atomization Particle Size of HPMC Aqueous Solutions. HPMC aqueous solutions with the same concentration (0.5%, w/w) were measured by means of a laser diffraction particle size analyzer (Winner319B, Jinan Weiner Particle Instrument Co., Ltd., China). The pump pressure, pump speed, and nozzle distance from the laser during the test process are 0.3 MPa, 50 rpm, and 49 cm, respectively. The diameters of the inner air holes, nozzles, and outer pores of the spray gun are 1.5, 4.5, and 7.5 mm, respectively. When V_{10}, V_{50}, and V_{90} were automatically achieved, the width of the atomized particle size distribution (S) was calculated by using the following equation

$$S = \frac{d_{V90} - d_{V10}}{d_{V50}} \tag{6}$$

where d_{V10}, d_{V50}, and d_{V90} represent the diameters of 10, 50, and 90% of the cumulative particle distributions, respectively.

4.4. SeDeM Characterization. The SeDeM expert system is an excellent preformulation method because it predicts the suitability of materials for direct compression and gathers almost all the frequently used physical parameters of pharmaceutical powders.[30] The different physical properties of HPMC powders (dimension, compressibility, powder flow,

https://doi.org/10.1021/acsomega.1c03009
ACS Omega 2021, 6, 28598−28610

Table 5. Parameters and Equations Used in the SeDeM Method[a]

incidence	parameter (symbol)	unit	equation	limit value	convert to radius value
dimension	bulk density (Da)	g/mL	Da = P/Va	0−1	10ν
	tapped density (Dc)	g/mL	Dc = P/Vc	0−1	10ν
compressibility	interparticle porosity (Ie)	-	Ie = (Dc − Da)/(Dc × Da)	0−1.2	10ν/1.2
	Carr index (IC)	%	IC = (DC − Da)/Dc × 100	0−50	ν/5
	cohesion index (Icd)	N	experimental	0−200	ν/20
powder flow	Hausner ratio (IH)	-	IH = Dc/Da	3−1	(30 − 10ν)/2
	angle of repose (α)	°	experimental	50−0	10 − (ν/5)
	flowability (t'')	s	experimental	20−0	10 − (ν/2)
stability	loss on drying (% HR)	%	experimental	10−0	10 − ν
	hygroscopicity (% H)	%	experimental	20−0	10 − (ν/2)
lubricity	particles < 50 μm (% Pf)	%	experimental	50−0	10 − (ν/5)
	homogeneity index (Iθ)	-	eq 13	0−0.02	500ν

[a]P, the weight of the powder to be measured; Va, the bulk volume of the powder; Vc, the tapped volume of the powder; N, the hardness of tablets; and ν, experimental values of parameters. $I\theta = F_m/[100 + (d_m - d_{m-1})F_{m-1} + (d_{m+1} - d_m)F_{m+1} + (d_m - d_{m-2})F_{m-2} + (d_{m+2} - d_m)F_{m+2} \ldots (d_{m+n} - d_m)F_{m+n}]$ where F_m is the percentage of particles in the majority range, F_{m-1} is the percentage of particles in the range immediately below the majority range, F_{m+1} is the percentage of particles in the range immediately above the majority range, n is the fraction under study, the order number within a series, with respect to the median fraction, d_m is the mean diameter of the particles in the majority fraction, d_{m-1} is the mean diameter of the particles in the fraction of the range immediately below the majority range, and d_{m+1} is the mean diameter of the particles in the fraction of the range immediately above the majority range.

stability, and lubricity) were investigated in this paper. According to the SeDeM method, the physical properties of HPMC powders were characterized by 12 parameters, as shown in Table 5.

4.4.1. Bulk Density. Approximately 15 g of each powder to be tested was slowly poured into a graduated 50 mL cylinder, and its volume was recorded. Da was calculated from the powder weight and the corresponding bulk volume.

$$\mathrm{Da} = \frac{P}{\mathrm{Va}} \tag{7}$$

where P is the weight of the powder and Va is the volume mark in the cylinder.

4.4.2. Tapped Density. The cylinder with the sample powder was knocked 1250 times in a tap density tester (BT-301, Dandong Baite Instrument Co., Ltd., China), and its tapped volume was recorded. Dc was calculated from the powder weight and the corresponding tapped volume.

$$\mathrm{Dc} = \frac{P}{\mathrm{Vc}} \tag{8}$$

where P is the weight of the powder and Vc is the volume mark in the cylinder after 1250 taps of the cylinder in the instrument.

4.4.3. Interparticle Porosity.

$$\mathrm{Ie} = \frac{\mathrm{Dc} - \mathrm{Da}}{\mathrm{Dc} \times \mathrm{Da}} \tag{9}$$

4.4.4. Carr Index.

$$\mathrm{IC} = \frac{\mathrm{Dc} - \mathrm{Da}}{\mathrm{Dc}} \times 100 \tag{10}$$

4.4.5. Cohesion Index. Icd is the mean hardness of tablets obtained by compressing powders under the maximum eccentric compression force. According to a proposed new methodology for determining the Icd parameter, the weight of a tablet is adjusted concerning its bulk density.[31] Tablet hardness was determined for five tablets that were prepared by a single impulse-type tablet machine (DP30A, Beijing Xinlongli Technology Co., Ltd., China). If any of the powders cannot be compressed due to bad flow of powder or excessive ejection force being required, a 3.5% w/w mixture including 2.36% of talc, 0.14% of Aerosil 200, and 1.00% of magnesium stearate should be added.[32]

4.4.6. Hausner Ratio. IH was obtained from Dc and Da according to the formula

$$\mathrm{IH} = \frac{\mathrm{Dc}}{\mathrm{Da}} \tag{11}$$

4.4.7. Angle of Repose. Using an angle of repose tester (HYL-105, Dandong Baite Instrument Co., Ltd., China), 100 g of the powder was injected into the horizontal tray (diameter φ 100 mm) from the funnel port (flow outlet diameter φ10 mm). According to the principle of the similar triangle, the angle of repose was determined directly by a protractor.

4.4.8. Flowability. Using a powder flow tester (BT-100, Dandong Baite Instrument Co., Ltd., China), 100 g of the powder was added to a funnel with a nozzle diameter of 10 mm. The channel was opened, and the time was recorded when all the powders pass through the funnel. If the powder does not pass through the funnel, it can be tested with a larger diameter (15 or 25 mm) nozzle.

4.4.9. Loss on Drying. % HR was measured through an infrared rapid moisture analyzer (SFY-60, Shenzhen Guanya Electronic Technology Co., Ltd., China). About 2 g of the sample was placed into the sample pan and heated for 10 min at 105 °C to record the moisture value finally displayed by the instrument.

4.4.10. Hygroscopicity. A dried stoppered glass weighing bottle was placed in a (22 ± 2) °C constant temperature dryer (saturated solution of sodium chloride in the lower part) and weighed accurately (m_1) after 12 h. An appropriate amount of the powder was tiled in the weighing bottle (about 1 mm thick) and the weighing cap was covered, with precision weighing (m_2). The weighing bottle was exposed and placed in the same constant temperature and humidity conditions as the cap.[33] After 24 h, the weighing bottle was weighed accurately together with the weighing cap (m_3). The formula for calculating % H is as follows. The mass gain was recorded in percentage.

https://doi.org/10.1021/acsomega.1c03009
ACS Omega 2021, 6, 28598−28610

$$\%\,\mathrm{H} = \frac{m_3 - m_2}{m_2 - m_1} \times 100\% \quad (12)$$

4.4.11. Particle Size < 50 μm. An appropriate amount of the powder was tiled in the dry sampler of a laser diffraction particle size analyzer (Mastersizer 3000, Malvern, England) with air as the dispersion medium. The percentage of particles that are no more than 0.05 mm was considered as % Pf.

4.4.12. Homogeneity Index. Iθ was measured using the laser diffraction particle size analyzer (Mastersizer 3000, Malvern, England) on a series of sieves (0.05, 0.100 0.212, and 0.355 mm). The percentage of particles in the major range (F_m) and the mean diameter (d_m) correspond to the interval from 0.100 to 0.212 mm. The percentage of the particles in the range below the major range (F_{m-1}) and the mean diameter (d_{m-1}) correspond to the interval from 0.05 to 0.100 mm. The percentage of the particles in the range above the major range (F_{m+1}) and the mean diameter (d_{m-1}) correspond to the interval from 0.212 to 0.355 mm. Iθ was calculated according to the following formula.

$$\mathrm{I}\theta = F_m/[100 + (d_m - d_{m-1})F_{m-1} + (d_{m+1} - d_m)F_{m+1} + (d_m - d_{m-2})F_{m-2} + (d_{m+2} - d_m)F_{m+2} \ldots (d_{m+n} - d_m)F_{m+n}] \quad (13)$$

where:

F_m: percentage of particles in the majority range

F_{m-1}: percentage of particles in the range immediately below the majority range

F_{m+1}: percentage of particles in the range immediately above the majority range

n: for the fraction under study, the order number within a series, with respect to the median fraction

d_m: mean diameter of the particles in the majority fraction

d_{m-1}: mean diameter of the particles in the fraction of the range immediately below the majority range

d_{m+1}: mean diameter of the particles in the fraction of the range immediately above the majority range

4.5. Tablet Characterization. Different batches of HPMC were compressed into tablets (200 mg weight) using a single impulse-type tablet machine (DP30A, Beijing Xinlongli Technology Co., Ltd., China) under the same conditions with 9.0 mm round, flat-faced punches. The tablets were compressed twice by a texture analyzer (CT3-10k, Brookfield, USA) under the mode of texture profile analysis. The test conditions include a cylindrical probe with a 4 mm diameter, the test speed is 1.0 mm/s, the trigger force is 1000 g, and the shape variable is 0.1 mm.

4.5.1. Tablet Hardness. Six tablets for each batch of HPMC were individually subjected to test using a texture analyzer, and the first cycle hardness is taken as HD.

4.5.2. Tensile Strength. For six tablets for each batch of HPMC, the diameter (D) and thickness (t) were gauged using a digital caliper (500-196-30 Digimatic Caliper, Mitutoyo, USA). The breaking force (F) was measured using a texture analyzer (CT3-10k, Brookfield, USA). TS of the tablets was calculated using the equation[34]

$$\mathrm{TS} = \frac{2F}{\pi D t} \quad (14)$$

4.6. Apparent Viscosity. An appropriate amount of the sample was added to 90 °C deionized water to make the same concentration of HPMC aqueous solutions (2%, w/w) and stirred thoroughly for about 10 min to disperse the particles uniformly. Then, HPMC aqueous solutions were cooled in an ice bath, and the upper bubbles were removed. The apparent viscosity was measured using a digital display viscometer (NDJ-5S, Shanghai Hengping Instrument Factory, China) at 20 °C at 60 rpm speed. The samples were measured in triplicate.

4.7. Statistical Variable Selection. In this study, 33 variables were selected for statistical analysis to understand the effect of each variable on 8 observations (representing 8 batches of HPMC with 2 manufacturers and 3 viscosity grades). The particle size distribution {d_{10}, d_{50}, d_{90}, D[3,2], D[4,3], BET, span, and width} of HPMC powders was an important factor for evaluating the quality attributes of HPMC products. The atomization particle size (d_{V10}, d_{V50}, d_{V90}, and S) of HPMC was also a key factor in determining wet granulation and in vitro dissolution. The smaller the atomization particle size of the droplet, the better the wet granulation effect and the more uniform the tablet coating. Therefore, the better the granulation effect, the more uniform the dissolution in vitro. The HPMC powder behavior was evaluated using 12 previously characterized indicators (Da, Dc, % Pf, IH, Iθ, α, t'', Ie, IC, Icd, % HR, and % H). Infrared spectral wavelengths corresponding to hydroxyl (σ_1), methylene (σ_2), primary alcohol (σ_3), crystal form ($2\theta_1$ and $2\theta_2$), and glass transition temperature (T_g) were used to determine whether different HPMC samples belong to the same material. In the quality analysis of HPMC, apparent viscosity (vis) was one of the important indicators of detection. The variables related to compression behavior were HD and TS, indicating that a certain mechanical strength is achieved by plastic or elastic deformation after significant appreciable interparticle bonding has taken place.

4.8. Data Processing and Statistical Analysis. Raw data of 33 variables were normalized to improve the model quality, classification accuracy, and interpretability of subsequent data. The normalized data set was imported into SIMCA 14.1 (Umetrics, Umeå Sweden) for multivariate analysis. The suitability of PCA and OPLS-DA models was evaluated before the analysis by cross-validation.[35] Based on VIP values > 1.0 obtained from the OPLS-DA model and p values < 0.05 acquired from the Student's test, a set of discriminating variables was determined.

AUTHOR INFORMATION

Corresponding Authors

Chuanyun Dai − *Chongqing Key Laboratory of Industrial Fermentation Microorganisms, School of Chemistry and Chemical Engineering, Chongqing University of Science and Technology, Chongqing 401331, China;* orcid.org/0000-0001-8890-3017; Phone: +86-23-65022212; Email: cydai@cqust.edu.cn, cydai@126.com

Huimin Sun − *NMPA Key Laboratory for Quality Research and Evaluation of Pharmaceutical Excipients, National Institutes for Food and Drug Control, Beijing 100050, China;* Phone: +86-10-53852486; Email: sunhm@126.com

Bochu Wang − *Key Laboratory of Biorheological Science and Technology, Ministry of Education, College of Bioengineering, Chongqing University, Chongqing 400030, China;* orcid.org/0000-0002-0592-3264; Phone: +86-23-65102507; Email: wangbc2000@126.com

https://doi.org/10.1021/acsomega.1c03009
ACS Omega 2021, 6, 28598−28610

Authors

Shulin Wan − *Chongqing Key Laboratory of Industrial Fermentation Microorganisms, School of Chemistry and Chemical Engineering, Chongqing University of Science and Technology, Chongqing 401331, China;* Present Address: Now pursuing the Ph.D. degree in School of Pharmacy, China Pharmaceutical University, Nanjing 210009, China

Yuling Bai − *Chongqing Key Laboratory of Industrial Fermentation Microorganisms, School of Chemistry and Chemical Engineering, Chongqing University of Science and Technology, Chongqing 401331, China*

Wenying Xie − *Chongqing Key Laboratory of Industrial Fermentation Microorganisms, School of Chemistry and Chemical Engineering, Chongqing University of Science and Technology, Chongqing 401331, China*

Tianbing Guan − *Chongqing Key Laboratory of Industrial Fermentation Microorganisms, School of Chemistry and Chemical Engineering, Chongqing University of Science and Technology, Chongqing 401331, China*

Complete contact information is available at: https://pubs.acs.org/10.1021/acsomega.1c03009

Author Contributions

The experimental design was contributed by C.D. and H.S., experimental studies were performed by S.W., analysis of results was done by S.W. and T.G., funding acquisition was done by C.D., H.S., and B.W., writing (manuscript draft preparation) was done by S.W., writing (review and editing) was done by C.D., and supervision and validation of results were performed by Y.B. and W.X. All authors have read and agreed to the published version of the manuscript.

Notes

The authors declare no competing financial interest.

■ ACKNOWLEDGMENTS

This work emanated from research conducted with the financial support of 2017 Sub-project 6 of National Major Scientific and Technological Special Project for "Significant New Drugs Development" of the Ministry of Science and Technology of China (2017ZX09101001006), Chongqing Technology Innovation and Application Development Project (cstc2020jscx-msxmX0048), and the Visiting Scholar Foundation of Key Laboratory of Biorheological Science and Technology (Chongqing University), the Ministry of Education (CQKLBST-2005001).

■ REFERENCES

(1) Fonteyne, M.; Wickström, H.; Peeters, E.; Vercruysse, J.; Ehlers, H.; Peters, B.-H.; Remon, J. P.; Vervaet, C.; Ketolainen, J.; Sandler, N.; Rantanen, J.; Naelapää, K.; Beer, T. D. Influence of Raw Material Properties upon Critical Quality Attributes of Continuously Produced Granules and Tablets. *Eur. J. Pharm. Biopharm.* **2014**, *87*, 252−263.

(2) Yu, L. X.; Amidon, G.; Khan, M. A.; Hoag, S. W.; Polli, J.; Raju, G. K.; Woodcock, J. Understanding Pharmaceutical Quality by Design. *AAPS J.* **2014**, *16*, 771−783.

(3) Tajarobi, F.; Abrahmsén-Alami, S.; Hansen, M.; Larsson, A. The Impact of Dose and Solubility of Additives on the Release from HPMC Matrix Tablets-Identifying Critical Conditions. *Pharm. Res.* **2009**, *26*, 1496−1503.

(4) Siow, C. R. S.; Tang, D. S.; Heng, P. W. S.; Chan, L. W. Probing the Impact of HPMC Viscosity Grade and Proportion on the Physical Properties of Co-Freeze-Dried Mannitol-HPMC Tableting Excipients Using Multivariate Analysis Methods. *Int. J. Pharm.* **2019**, *556*, 246−262.

(5) Han, J. K.; Shin, B. S.; Choi, D. H. Comprehensive Study of Intermediate and Critical Quality Attributes for Process Control of High-Shear Wet Granulation Using Multivariate Analysis and the Quality by Design Approach. *Pharmaceutics* **2019**, *11*, 252.

(6) Savaşer, A.; Taş, Ç.; Bayrak, Z.; Özkan, C. K.; Özkan, Y. Effect of Different Polymers and Their Combinations on the Release of Metoclopramide HCl from Sustained-Release Hydrophilic Matrix Tablets. *Pharm. Dev. Technol.* **2013**, *18*, 1122.

(7) Li, C. L.; Martini, L. G.; Ford, J. L.; Roberts, M. The Use of Hypromellose in Oral Drug Delivery. *J. Pharm. Pharmacol.* **2005**, *57*, 533.

(8) Nokhodchi, A.; Ford, J. L.; Rowe, P. H.; Rubinstein, M. H. The Effects of Compression Rate and Force on the Compaction Properties of Different Viscosity Grades of Hydroxypropylmethylcellulose 2208. *Int. J. Pharm.* **1996**, *129*, 21−31.

(9) Ford, J. Thermal Analysis of Hydroxypropylmethylcellulose and Methylcellulose: Powders, Gels and Matrix Tablets. *Int. J. Pharm.* **1999**, *179*, 209−228.

(10) Williams, R. O.; Sykora, M. A.; Mahaguna, V. Method to Recover a Lipophilic Drug from Hydroxypropyl Methylcellulose Matrix Tablets. *AAPS PharmSciTech* **2001**, *2*, 29−37.

(11) Tank, D.; Karan, K.; Gajera, B. Y.; Dave, R. H. Investigate the Effect of Solvents on Wet Granulation of Microcrystalline Cellulose Using Hydroxypropyl Methylcellulose as a Binder and Evaluation of Rheological and Thermal Characteristics of Granules. *Saudi Pharm. J.* **2018**, *26*, 593−602.

(12) Zhou, D.; Law, D.; Reynolds, J.; Davis, L.; Smith, C.; Torres, J. L.; Dave, V.; Gopinathan, N.; Hernandez, D. T.; Springman, M. K.; Zhou, C. C. Understanding and Managing the Impact of HPMC Variability on Drug Release from Controlled Release Formulations. *J. Pharm. Sci.* **2014**, *103*, 1664−1672.

(13) Ishizuka, Y.; Ueda, K.; Okada, H.; Takeda, J.; Karashima, M.; Yazawa, K.; Higashi, K.; Kawakami, K.; Ikeda, Y.; Moribe, K. Effect of Drug-Polymer Interactions through Hypromellose Acetate Succinate Substituents on the Physical Stability on Solid Dispersions Studied by Fourier-Transform Infrared and Solid-State Nuclear Magnetic Resonance. *Mol. Pharm.* **2019**, *16*, 2785−2794.

(14) Vanhoorne, V.; Janssens, L.; Vercruysse, J.; De Beer, T.; Remon, J. P.; Vervaet, C. Continuous Twin Screw Granulation of Controlled Release Formulations with Various HPMC Grades. *Int. J. Pharm.* **2016**, *511*, 1048−1057.

(15) Piriyaprasarth, S.; Sriamornsak, P. Effect of Source Variation on Drug Release from HPMC Tablets: Linear Regression Modeling for Prediction of Drug Release. *Int. J. Pharm.* **2011**, *411*, 36−42.

(16) Roopwani, R.; Buckner, I. S. Understanding Deformation Mechanisms during Powder Compaction Using Principal Component Analysis of Compression Data. *Int. J. Pharm.* **2011**, *418*, 227−234.

(17) Tadwee, I.; Shahi, S. Formulation Development of Losartan Potassium Immediate Release Tablets and Process Optimization Using SeDeM Expert System. *J. Appl. Pharm. Sci.* **2018**, *8*, 033−043.

(18) Mishra, A.; Vuddanda, P. R.; Singh, S. Intestinal Lymphatic Delivery of Praziquantel by Solid Lipid Nanoparticles: Formulation Design, in Vitro and in Vivo Studies. *J. Nanotechnol.* **2014**, *2014*, 1−12.

(19) Song, M.; Hammiche, A.; Pollock, H. M.; Hourston, D. J.; Reading, M. Modulated Differential Scanning Calorimetry: 4. Miscibility and Glass Transition Behaviour in Poly(Methyl Methacrylate) and Poly(Epichlorohydrin) Blends. *Polymer* **1996**, *37*, 5661−5665.

(20) Zhang, Y.; Che, E.; Zhang, M.; Sun, B.; Gao, J.; Han, J.; Song, Y. Increasing the Dissolution Rate and Oral Bioavailability of the Poorly Water-Soluble Drug Valsartan Using Novel Hierarchical Porous Carbon Monoliths. *Int. J. Pharm.* **2014**, *473*, 375−383.

(21) Varatharajan, R.; Manogaran, G.; Priyan, M. K. A Big Data Classification Approach Using LDA with an Enhanced SVM Method for ECG Signals in Cloud Computing. *Multimed. Tool. Appl.* **2018**, *77*, 10195−10215.

(22) Haware, R. V.; Tho, I.; Bauer-Brandl, A. Application of Multivariate Methods to Compression Behavior Evaluation of Directly Compressible Materials. *Eur. J. Pharm. Biopharm.* **2009**, *72*, 148−155.
(23) Lei, H.; Zhang, Y.; Ye, J.; Cheng, T.; Liang, Y.; Zu, X.; Zhang, W. A Comprehensive Quality Evaluation of Fuzi and Its Processed Product Through Integration of UPLC-QTOF/MS Combined MS/MS-based Mass Spectral Molecular Networking with Multivariate Statistical Analysis and HPLC-MS/MS. *J. Ethnopharmacol.* **2021**, *266*, 113455.
(24) Zhang, Q.; Feng, F. The Effects of Different Varieties of Aurantii Fructus Immaturus on the Potential Toxicity of Zhi-Zi-Hou-Po Decoction Based on Spectrum-Toxicity Correlation Analysis. *Molecules* **2019**, *24*, 4254.
(25) Wang, Y.-Q.; Li, S.-J.; Man, Y.-H.; Zhuang, G. Serum Metabonomics Coupled with HPLC-LTQ/orbitrap MS and Multivariate Data Analysis on the Ameliorative Effects of Bidens bipinnata L. in Hyperlipidemic Rats. *J. Ethnopharmacol.* **2020**, *262*, 113196.
(26) Tundisi, L. L.; Mostaço, G. B.; Carricondo, P. C.; Petri, D. F. S. Hydroxypropyl Methylcellulose: Physicochemical Properties and Ocular Drug Delivery Formulations. *Eur. J. Pharm. Sci.* **2021**, *159*, 105736.
(27) Chang, S.-Y.; Sun, C. C. Superior Plasticity and Tabletability of Theophylline Monohydrate. *Mol. Pharm.* **2017**, *14*, 2047−2055.
(28) Zhang, Y.; Xu, B.; Wang, X.; Dai, S.; Sun, F.; Ma, Q.; Shi, X.; Qiao, Y. Setting up Multivariate Specifications on Critical Raw Material Attributes to Ensure Consistent Drug Dissolution from High Drug-Load Sustained-Release Matrix Tablet. *Drug Dev. Ind. Pharm.* **2018**, *44*, 1733−1743.
(29) Sahu, A. K.; Jain, V. Screening of Process Variables Using Plackett−Burman Design in the Fabrication of Gedunin-Loaded Liposomes. *Artif. Cells, Nanomed., Biotechnol.* **2017**, *45*, 1011−1022.
(30) Aguilar-Díaz, J. E.; García-Montoya, E.; Pérez-Lozano, P.; Suñé-Negre, J. M.; Miñarro, M.; Ticó, J. R. SeDeM Expert System a New Innovator Tool to Develop Pharmaceutical Forms. *Drug Dev. Ind. Pharm.* **2014**, *40*, 222−236.
(31) Nofrerias, I.; Nardi, A.; Suñé-Pou, M.; Boeckmans, J.; Suñé-Negre, J. M.; García-Montoya, E.; Pérez-Lozano, P.; Ticó-Grau, J. R.; Miñarro-Carmona, M. Optimization of the Cohesion Index in the Sedem Diagram Expert System and Application of Sedem Diagram: An Improved Methodology to Determine the Cohesion Index. *PLoS One* **2018**, *13*, No. e0203846.
(32) Hamman, H.; Hamman, J.; Wessels, A.; Scholtz, J.; Steenekamp, J. H. Development of Multiple-Unit Pellet System Tablets by Employing the SeDeM Expert Diagram System I: Pellets with Different Sizes. *Pharm. Dev. Technol.* **2018**, *23*, 706−714.
(33) Sunenegre, J.; Perezlozano, P.; Miñarro, M.; Roig, M.; Fuster, R.; Hernández, C.; Ruhí, R.; Garciamontoya, E.; Ticó, J. Application of the SeDeM Diagram and a New Mathematical Equation in the Design of Direct Compression Tablet Formulation. *Eur. J. Pharm. Biopharm.* **2008**, *69*, 1029−1039.
(34) Fell, J. T.; Newton, J. M. Determination of Tablet Strength by the Diametral-compression Test. *J. Pharm. Sci.* **1970**, *59*, 688−691.
(35) Otsuka, T.; Iwao, Y.; Miyagishima, A.; Itai, S. Application of Principal Component Analysis Enables to Effectively Find Important Physical Variables for Optimization of Fluid Bed Granulator Conditions. *Int. J. Pharm.* **2011**, *409*, 81−88.

https://doi.org/10.1021/acsomega.1c03009
ACS Omega 2021, 6, 28598−28610